Self-consistent meson coupling calculations

Ernesto A. Matute
Departamento de Física, Facultad de Ciencia, Universidad de Santiago de Chile, Casilla 5659-Correo 2, Santiago, Chile
(Received 14 May 1985)

A recently developed self-consistent technique, based on analyticity, unitarity, and generalized ladder-graph dynamics, is used to calculate soft-meson couplings. Ladder exchanges are approximated by Regge exchanges and certain duality constraints are imposed, leading to ρ-, f-, and g-meson $\pi\pi$ partial decay widths which are in good agreement with the data. If the dual-tree approximation for the triple-Regge vertex $g(t,t',t'')$ is made, a value for $g(0,0,0)$ in reasonable agreement with experiment is obtained.

I. INTRODUCTION

The usual approaches to different kinds of hadronic calculations in the confinement region neglect $\bar{q}q$ creation and annihilation in first approximation. This is sometimes justified on the basis of the N_f/N_c expansion of QCD, with the number of flavors N_f fixed when the number of colors $N_c \to \infty$ (Ref. 1). However, this limit is a very unrealistic approximation to a world with $N_c=3$ and $N_f=3$ even for light quarks, so that $\bar{q}q$ effects could be important. As a matter of fact, sea quarks, which arise from $\bar{q}q$ creation, are known to play an important role for small fractional quark momenta (or Feynman-x values) within hadrons in deep-inelastic lepton-hadron scattering experiments. Since small x corresponds to the crucial long-range part of the confinement region, there is every reason to expect that a realistic soft-hadron physics will emerge only when $\bar{q}q$ effects are properly taken into account. The usual difficulties with chiral symmetry and in accounting for the smallness of the pion mass are undoubtedly manifestations of this fact. A standard way of overcoming such difficulties is to assume a chiral bag or cloudy bag model,[2] in which a cloud of mesons surrounds a core of valence quarks—a picture which also leads naturally to the successful meson-exchange description of nuclear forces. But the existence of such a cloud of mesons is only possible if a "hadronization," arising from $\bar{q}q$ creation, takes place.

The dual topological unitarization (DTU) program[3–5] is a highly promising fundamental approach to soft-hadron physics, in which sea quarks play an indispensable role from the beginning. Their hadronization implies that strong interactions between hadrons in the low-momentum-transfer (or long-distance) regime are mediated by $\bar{q}q$ mesons, qqq baryons, and $\bar{q}\bar{q}qq$ baryonium.

Earlier versions of DTU, while unambiguous and successful for mesons, could not consistently take into account baryons and baryonium states.[3] However, the generalized scheme of Chew and Poénaru[4] and Stapp[5] provides a consistent way of overcoming this difficulty, without modifying in any way the meson sector. In their approach, one or more quark lines can be replaced by "diquarks" of a certain well-defined topological structure, and "Landau" lines, which are associated with the four-momenta of hadrons in any given diagram, are introduced. It can be argued that the "interactions" of the Landau lines with the diquarks must be weak. As a consequence, diquark breakup and formation, and therefore baryonium $\leftrightarrow$ meson transitions, are forbidden in first approximation, so that baryonium states should be narrow below the baryon-antibaryon threshold.

At the lowest level of the Chew-Poénaru-Stapp scheme, spin-momentum coupling is dealt approximately and parity is violated. In this paper, however, we shall work at a more accurate lowest level in which baryonium $\leftrightarrow$ meson transitions remain suppressed, but in which parity is satisfied and the spin and momentum are properly coupled to each other; all of our considerations will be limited to mesons only.

The DTU scheme provides a method of quasiperturbative expansion to calculate the scattering amplitude for the different quark-duality diagrams generated by unitarity. These diagrams are ordered according to their topological complexity. Thus for meson-meson scattering in the flavor-SU(N_f) scheme, the leading term is the planar amplitude, which corresponds to the sum of all the planar (uncrossed) quark-duality diagrams of Fig. 1, at least if we neglect diquark-loop diagrams, which have the same form as the diagrams of Fig. 1, but with the internal q lines replaced by $\bar{\delta}=\bar{q}\bar{q}$ lines. These correspond to nonmeson intermediate-state channels which involve lower-lying Regge trajectories and should therefore be less important. The first-order correction is the cylinder term, which corresponds to the nonplanar (crossed) quark-duality diagrams of Fig. 2, where again we neglect diquark internal lines.

In the above unitary sums, we can count the powers of

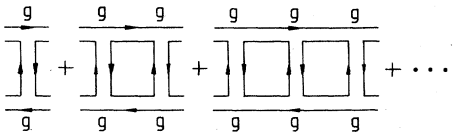

FIG. 1. The sum of planar quark-duality diagrams for a meson + meson → meson + meson process.

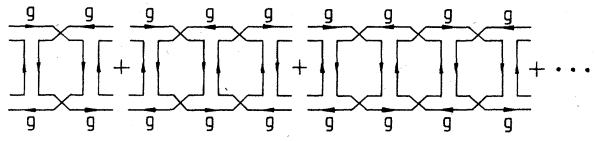

FIG. 2. The sum of cylinder quark-duality diagrams for a meson + meson→meson + meson process.

the coupling constant for each planar diagram as g^2, $g^2(g^2N_f)$, $g^2(g^2N_f)^2$, ..., where N_f comes from the flavor sum for each quark loop; similarly, for the cylinder diagrams, we see that they go as g^4, $g^4(g^2N_f)$, $g^4(g^2N_f)^2$, ..., where the factor N_f again comes from the fact that each quark loop can take on N_f different flavors. If we take the $g^2N_f \sim 1$ bootstrap constraint,[6,3] each term of the summation has the same order of $1/N_f$, i.e., $g^2 \sim 1/N_f$ for the planar and $g^4 \sim 1/N_f{}^2$ for the cylinder diagrams. For more complex quark diagrams, the order of $1/N_f$ for an amplitude is determined by the topology of the diagrams. In general the contribution of any quark-duality diagram becomes weaker as its topology gets more complicated.[3]

If we only keep the contribution of the planar diagrams to the full 2→2 scattering amplitude, we can consistently obtain the "planar unitarity" equation

$$2\,\mathrm{Im}T_{12\to 34}(\text{planar}) = \sum_n T_{12\to n}(\text{planar})T^{\dagger}_{34\to n}(\text{planar}) , \tag{1.1}$$

where the summation is over all possible intermediate states. The two planar amplitudes are "joined" to each other in such a way that there are no crossed lines, as illustrated in Fig. 3. Equation (1.1) constitutes a highly nonlinear constraint for the amplitude T. Its solution is a self-consistent scattering amplitude, in the sense that the output T exactly coincides with the input T.

The above planar bootstrap problem is the first step in the DTU program. Once we have its solution, nonplanar effects can then be systematically brought in through the topological expansion. Up to now, however, we do not have any explicit theory which defines the exact form of the planar amplitude. Therefore, in practical calculations, one relies on some kind of approximation or assumption about the form of the amplitude. In the present work we shall use the self-consistent DTU technique developed by Balázs in Refs. 7 and 8, which has been successfully applied to $\bar{q}q$, qqq, and $\bar{q}\bar{q}qq$ hadrons.

In Sec. II we review the dynamical considerations of Balázs's approach. In Sec. III we construct a model to make coupling calculations. We compute the triple-Regge coupling constant and meson couplings. For simplicity we consider only $\pi\pi$ scattering. Then we compare the results with similar calculations based on a dual-tree model of the Neveu-Schwartz type and with experiment. Our conclusions are summarized in Sec. IV.

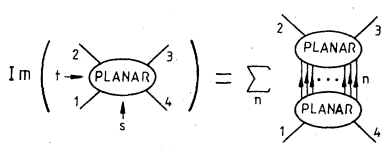

FIG. 3. Planar unitarity as given by Eq. (1.1).

II. DYNAMICAL CONSTRAINTS

The simplest way of implementing planar unitarity is to represent the amplitude T by an infinite sum of ladder graphs.[9,10] If we also assume that particles are produced in clusters (resonances), so that the sum over n in Eq. (1.1) can be rewritten as a sum over clusters, Fig. 3 takes on the form shown in Fig. 4. For large s each ladder line may be approximated by a Regge exchange $\alpha(t)$.[11] The requirement that there be no double-counting, say, between Figs. 4(a) and 4(b), implies that the clusters $(a,\ldots)$, $(b,\ldots)$, $(c,\ldots)$ must be bounded; they are therefore dominated by bound states and resonances, which, in practical calculations, will be approximated by narrow-resonance peaks.

The evaluation of Fig. 4 entails a self-consistency problem (planar bootstrap), because the output Regge pole $\alpha(t)$ generated by the infinite sum of ladder graphs must be consistent with the input pole satisfying the duality relation of Fig. 5.

We will deal with the "ordered" planar amplitude $T(s,t)$ which only has s-t crossing symmetry and satisfies unitarity at the planar level.[3] The full planar amplitude is then a linear combination of $T(s,t)$, $T(s,u)$, and $T(t,u)$, where s, t, and u are the Mandelstam variables.

To handle the graphs of Fig. 4, we formally associate a coupling-strength parameter ϕ with each of the clusters $(a,\ldots)$, $(b,\ldots)$, $(c,\ldots)$, ..., and make the Mellin-transform projection

$$A_j(t) = \int_0^\infty d\nu\, A(s,t)\nu^{-j-1} , \tag{2.1}$$

where ν is the usual crossing-symmetric variable $(s-u)/2$, which can also be written as

$$\nu = s + \frac{1}{2}\left[t - \sum_{i=1}^{4} m_i{}^2\right] . \tag{2.2}$$

Thus the projected sum of Fig. 4 takes on the form of an expansion in ϕ:

$$A_j(t) = \phi a_{1j}(t) + \phi^2 a_{2j}(t) + \phi^3 a_{3j}(t) + \cdots , \tag{2.3}$$

where $\phi a_{1j}(t)$ is the Mellin transform of Fig. 4(a), which gives, approximately, a contribution to $A(\nu,t)$ of

$$\phi a_1(s,t) = \Gamma_a(t)\delta(s-s_a) + b_1(t)b_2(t)(\beta_0\nu)^{\alpha(t)}\Theta(s-\bar{s})\Theta(s_0-s) , \tag{2.4}$$

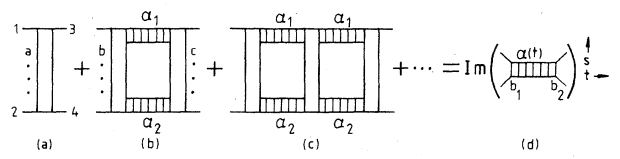

FIG. 4. Planar unitarity in terms of ladder graphs. For large s the ladder lines can be approximated by Regge exchanges. This infinite sum of ladder graphs has the same planar topological structure as the sum illustrated in Fig. 1.

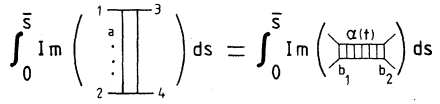

FIG. 5. Average duality relation between the cluster $(a,\ldots)$ and the Reggeon $\alpha(t)$.

where $(s_a)^{1/2}$ is the mass of the lowest nonvanishing contribution in Fig. 4(a) and $\bar{s}$ corresponds to a point approximately halfway between a and the next contribution above it. The δ-function term is then an approximation to the contribution of a and the Regge term $b_1 b_2 \nu^\alpha$ takes into account all the higher $s > \bar{s}$ contributions in the average sense of Fig. 5. To avoid a situation where the units of $b_1 b_2$ vary with $\alpha(t)$, we have introduced a scale factor β_0, with the same units as s^{-1}, so that $b_1 b_2$ become dimensionless. We will take the empirical value[11] $\beta_0 = 1\ \mathrm{GeV}^{-2}$; it will be omitted from the equations. Furthermore, since we are insisting on no double-counting between Figs. 4(a) and 4(b), we have inserted a step function $\Theta(s_0 - s)$ to exclude states above the effective threshold $s = s_0$ of Fig. 4(b). The remaining terms in Eq. (2.3) involve difficult loop integrals. We will discuss below some dynamical approximations that are useful in dealing with them.

If we take the $[1,N]$ Padé approximant[12] of Eq. (2.3) we obtain, for a given t,

$$A_j = \frac{\phi a_{1j}}{1 - K(j)} , \tag{2.5}$$

where

$$K(j) = \phi \frac{a_{2j}}{a_{1j}} + \phi^2 \left[\frac{a_{3j}}{a_{1j}} - \left[\frac{a_{2j}}{a_{1j}} \right]^2 \right] + \cdots \tag{2.6}$$

has N terms adjusted so that an expansion of Eq. (2.5) in powers of ϕ reproduces the first $(N+1)$ terms of Eq. (2.3). In the case of the lowest elastic process for a given set of quantum numbers, Eq. (2.5) satisfies elastic t-channel unitarity exactly for any finite value of N (see Ref. 8). We thus expect the series (2.6) to converge fairly rapidly in the limit $N \to \infty$. If we use the Mellin transform (2.1) we find, order by order, that Eq. (2.6) has the structure

$$K(j) = \int_{y_0}^{\infty} dy\, G(y) y^{-j-1} , \tag{2.7}$$

where $y = \nu/\nu_a$ and ν_a and ν_0 are the values of ν at $s = s_a$ and s_0, respectively.

From Eq. (2.5), A_j has a Regge pole at $j = \alpha$ if

$$K(\alpha) = 1 . \tag{2.8}$$

The corresponding residue, normalized as in Eq. (2.4), is

$$b_1 b_2 = -\phi a_{1\alpha} / K'(\alpha) . \tag{2.9}$$

We next require that the Regge pole satisfy the finite-energy sum rule[13] (FESR) of Fig. 5:

$$\int_0^{\bar{s}} ds [\phi a_1(\nu,t) - b_1(t) b_2(t) \nu^{\alpha(t)} \Theta(\nu)] \nu^{-S_1 - S_2} = 0 , \tag{2.10}$$

where S_1 and S_2 are the spins of the external particles. Equation (2.10) implies that the resonance average over $[0,\bar{s}]$ immediately constrains the high-energy Regge behavior, and conversely it ensures that the smooth Regge amplitude at high energies, if extrapolated to low energies, gives an average description of the behavior in the resonance region. Equation (2.10) is often referred to as semi-local duality.

If we apply (2.1) to (2.4), use (2.8) and (2.9), and combine with (2.10) and (2.7), we obtain

$$\frac{1}{\alpha + 1 - S_1 - S_2} \left[\frac{\bar{\nu}}{\nu_a} \right]^{\alpha + 1 - S_1 - S_2} + \ln \left[\frac{\nu_0}{\bar{\nu}} \right] = \frac{\int_{y_0}^{\infty} dy\, G(y) y^{-\alpha - 1} \ln y}{\int_{y_0}^{\infty} dy\, G(y) y^{-\alpha - 1}} . \tag{2.11}$$

The dynamics of our problem is now contained entirely within the function $G(y)$. If we take the discontinuity of Fig. 4(b) across the two-body intermediate state, as shown in Fig. 6(a), we have the two-Reggeon behavior $G(y) \propto y^{\alpha_{\mathrm{cut}}}$ for large y, modulo logarithmic factors.[9,14,15] On the other hand, by including higher intermediate states, such as the cut across a three-body intermediate state in Fig. 6(b), the $y^{\alpha_{\mathrm{cut}}}$ behavior is canceled for large y, leading to a sharp falloff in y.[11] We therefore expect the peaked structure of Fig. 7. This peaking permits us, in turn, to make the approximation

$$\ln y \simeq \ln(\nu_1/\nu_a) \tag{2.12}$$

within the integral of Eq. (2.11), with an α-independent α_1. Then Eq. (2.12) reduces (2.11) to the equation

$$e^X = C_1 X , \tag{2.13}$$

where

$$X = (\alpha + 1 - S_1 - S_2) \ln(\bar{\nu}/\nu_a) \tag{2.14}$$

and

$$C_1 = 1 + \frac{\ln(\nu_1/\nu_0)}{\ln(\bar{\nu}/\nu_a)} . \tag{2.15}$$

Since C_1 is independent of α, and hence of X, Eq. (2.13) will, in general, have up to two solutions for X, and hence for α. A more accurate treatment of Fig. 4 must be equivalent to a relativistic generalization of a multichannel, multiparticle version of a Lippmann-Schwinger or Schrödinger equation, however, and is therefore expected to give a unique output $\alpha(t)$. If we assume that this is in fact the case, $Y = C_1 X$ must be tangent to $Y = e^X$. This

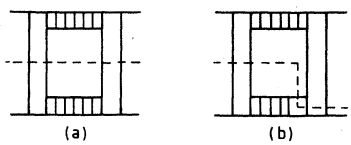

FIG. 6. (a) Figure 4(b) cut across the two-body intermediate state. (b) A cut across a three-body state.

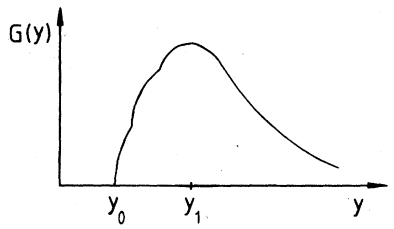

FIG. 7. The peaked structure of $G(y)$. The slope discontinuities result from the threshold effect of the successive opening up of the different s-channel intermediate-state channels associated with Figs. 4(b), 4(c),. . . .

gives

$$C_1=e,\quad X=1 \tag{2.16}$$

or, using Eqs. (2.14) and (2.15),

$$\nu_1=\nu_0(\bar{\nu}/\nu_a)^{e-1}$$
$$=\nu_0(\nu_a/\bar{\nu})\exp[e/(\alpha+1-S_1-S_2)]\ , \tag{2.17}$$

$$\alpha(t)=S_1+S_2-1+\left[\ln\left[1+\frac{\bar{s}-s_a}{\nu_a}\right]\right]^{-1}\ . \tag{2.18}$$

Equation (2.18) has branch points at $\nu_a=0$ and $\nu_a=-(\bar{s}-s_a)$, which can be joined by a cut in the ν_a plane. It can be argued[8] that this singularity structure is spurious and that the approximation (2.12), and hence Eq. (2.18), are not valid in that region. Away from this singular region, on the other hand, Eq. (2.18) can be well approximated by the linear expression

$$\alpha(t)=S_1+S_2+c+2\alpha'\nu_a\ , \tag{2.19}$$

a form which exactly reproduces the $t\to\infty$ Eq. (2.18) limits of $\alpha'(t)$ and $[\alpha(t)-t\alpha'(\infty)]$ if we take

$$c=-\tfrac{1}{2},\quad 2\alpha'=1/(\bar{s}-s_a)\ . \tag{2.20}$$

Equation (2.20) gives

$$\bar{s}=s_a+\tfrac{1}{2}\alpha'^{-1}\ . \tag{2.21}$$

For processes in which the s- and t-channel Regge slopes are equal, this is consistent with the usual semilocal-duality statement that $\bar{s}$ be at a point halfway between a and its first Regge recurrence. This would be the case for crossing-symmetric processes, for example, in which a lies on $\alpha(t)$ and α'^{-1} is the spacing between recurrences.

Using Eqs. (2.2) and (2.20), Eq. (2.19) can also be written as

$$\alpha(t)=S_1+S_2-\tfrac{1}{2}+2\alpha'\left[s_a+\frac{1}{2}\left[t-\sum_{i=1}^{4}m_i^2\right]\right]\ . \tag{2.22}$$

Equation (2.18) or Eq. (2.22) apply to a given specific process. The same output α can, however, arise in an infinite number of other processes. It turns out that consistency can be used to justify Eq. (2.22) for all t (Ref. 8). The same arguments do not apply to Eq. (2.18), and so we shall use only Eq. (2.22) in what follows.

Balázs[7,8] has applied (2.22), in a self-consistent way, to compute the low-mass hadron spectrum and the parameters of Regge trajectories. For example, for the Regge recurrences (i.e., orbital excitations) of π and ρ, with $m_\rho=0.776$ GeV fixing the scale, the following results are obtained:

$$m_\pi^2=m_\rho^2-(2\alpha'_\rho)^{-1}=0\ , \tag{2.23a}$$

$$\alpha_\pi(0)=0,\quad \alpha_\rho(0)=0.5\ , \tag{2.23b}$$

and

$$\alpha'_\pi=\alpha'_\rho=0.83\ \text{GeV}^{-2}\ , \tag{2.23c}$$

which are in good agreement with the experimental values.

III. PLANAR SELF-CONSISTENT CALCULATIONS OF COUPLINGS

The Regge-trajectory result (2.22) was based on the dynamical approximation (2.12), which might be expected to arise in a wide class of models. When applied to entire sets of processes, Eq. (2.22) gives powerful self-consistency conditions which determine the parameters of the Regge trajectories. On the other hand, coupling calculations inevitably require a more detailed model.

We will assume that Fig. 6(a) begins to be canceled by Fig. 6(b) only at relatively high values of s. Therefore we can approximate Fig. 4(b) by Fig. 6(a) when we evaluate a_{2j}. We will also approximate the ladder exchanges of Fig. 6(a) by Regge exchanges and assume that the [1,1] Padé approximant is a good representation of Eq. (2.5), so that Eq. (2.6) becomes

$$K(j)=\phi a_{2j}/a_{1j}\ , \tag{3.1}$$

with $\phi^2 a_{2j}$ given by Fig. 8. The practical advantage of using this approximant is that we only have to evaluate the first two diagrams of the sum of Fig. 4 explicitly. Moreover, in the case of factorizable models[10] the approximant is in fact exact. For simplicity, we will only consider $\pi\pi\to\pi\pi$ scattering.

A. Dynamical constraints at and near the forward direction

In the derivation of the Regge-trajectory formula (2.22), we obtained two dynamical constraints, namely, Eq. (2.8), which with the approximation (3.1), becomes

$$K(\alpha(t),t)=\phi a_{2\alpha(t)}(t)/a_{1\alpha(t)}(t)=1\ , \tag{3.2}$$

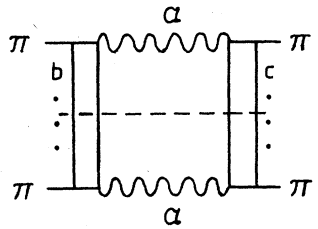

FIG. 8. Figure 6(a) for $\pi\pi\to\pi\pi$ in the Regge-exchange approximation.

and

$$\frac{1}{K(\alpha(t),t)}\left[\frac{\partial}{\partial j}K(j,t)\right]_{j=\alpha(t)} = -\ln\frac{\nu_1(t)}{\nu_a(t)} = -\frac{e}{1+\alpha(t)} - \ln\frac{\nu_0(t)}{\bar{\nu}(t)}\,, \quad (3.3)$$

which follows from Eqs. (2.7), (2.12), and (2.17) for $\pi\pi$ scattering.

In practice, $a_2(s,t)$ involves a double integral for $t\neq 0$. However, $a_2(s,0)$ and $[\partial a_2(s,t)/\partial t]_{t=0}$ can both be reduced to single integrals, so that our calculations will be made at and near $t=0$. Now one can assume a linear upper cutoff $\hat{s}_0(t)$, at least for small t, for the cluster $(b,\ldots)=(c,\ldots)$ of Fig. 4(b) or Fig. 8, which is different from the cutoff s_0 for the cluster $(a,\ldots)$ of Fig. 4(a). The latter will be assumed to be t independent. Allowing $\hat{s}_0$ to be t dependent, on the other hand, would be a crude way of taking higher ladder graphs into account more completely. If we now consider the constraints given by Eqs. (3.2), (3.3), and their t derivatives at $t=0$, we can determine the basic unknowns s_0, $\hat{s}_0(0)$, $\hat{s}_0'(0)$, and the overall normalization of our couplings. The expressions for the t derivatives at $t=0$ of (3.2) and (3.3) are

$$\alpha'(0)\left[\frac{\partial}{\partial j}K(j,0)\right]_{j=\alpha(0)} + \left[\frac{\partial}{\partial t}K(\alpha(0),t)\right]_{t=0} = 0 \quad (3.4)$$

and

$$\alpha'(0)\left[\frac{\partial^2}{\partial j^2}K(j,0)\right]_{j=\alpha(0)} + \left[\frac{\partial^2}{\partial t\,\partial j}K(j,t)\right]_{\substack{j=\alpha(0)\\ t=0}} = -\left[\frac{d}{dt}\ln\frac{\nu_1(t)}{\nu_a(t)}\right]_{t=0}. \quad (3.5)$$

B. A many-peaks approximation to the dynamical equations

The next step in our calculations is to find explicit representations for $\phi a_1(s,t)$ and $\phi^2 a_2(s,t)$.

For the crossing-symmetric $\pi\pi\to\pi\pi$ process, in which $a=\rho$ lies on $\alpha(t)$ and α'^{-1} is the spacing between recurrences, we can approximate the different contributions in $(a,\ldots)$ by narrow peaks at $s=m_{a(0)}^2$, $m_{a(1)}^2$, $m_{a(2)}^2,\ldots$ with $a(0)=a=\rho$ and a spacing $1/\alpha'$ between them. To relate the couplings of these states to each other, we make use of the FESR duality of Fig. 5 [see also Eq. (2.10)], which gives

$$\gamma_{\pi a\pi}^2(t) = \int_0^{\bar{\nu}_1} d\nu\,\gamma_{\pi\pi\alpha}^2(t)\nu^{\alpha(t)} \quad (3.6)$$

and

$$\gamma_{\pi a(n)\pi}^2(t) = \int_{\bar{\nu}_n}^{\bar{\nu}_{n+1}} d\nu\,\gamma_{\pi\pi\alpha}^2(t)\nu^{\alpha(t)}\Theta(s_0-s)\,, \quad (3.7)$$

where

$$\nu = s + \frac{t}{2} \quad (2.2')$$

and $\bar{\nu}_n$ is the value of ν at $s=\bar{s}_n$, with $\bar{s}_n$ midway between $s_{a(n-1)}$ and $s_{a(n)}$ for $n\geq 1$, and defined by

$$\bar{s}_n = s_a + (n-\tfrac{1}{2})\alpha'^{-1}\,. \quad (3.8)$$

We now consider the value $n=N$ such that $\bar{s}_N \leq s_0 \leq \bar{s}_{N+1}$. We will approximate the continuum between $\bar{s}_N$ and s_0 by a peak at $s=s_{a(N)}$ with a magnitude that is proportional to the length of the interval $[\bar{s}_N, s_0]$. Thus we have

$$\phi a_1(s,t) = \sum_{n=0}^{N} K_n \gamma_{\pi a(n)\pi}^2(t)\delta(s-s_{a(n)})\,, \quad (3.9)$$

with K_n defined by

$$K_n = \begin{cases} 1 & \text{if } n<N\,, \quad (3.10a)\\ \dfrac{s_0-\bar{s}_N}{\bar{s}_{N+1}-\bar{s}_N} & \text{if } n=N\,, \quad (3.10b)\end{cases}$$

which, in general, takes values between zero and one.

Similarly, we approximate the different states in $(b,\ldots)=(c,\ldots)$ by narrow peaks at $s=m_{b(0)}$, $m_{b(1)}$, $m_{b(2)},\ldots$ with $b(0)=b=\pi$ and a spacing α'^{-1} between them. We then have the generalized finite-energy sum rules of Fig. 9; this, under the assumption that the coupling of internal to external lines is factorizable, gives

$$\gamma_{\pi b\alpha}(t')\gamma_{\pi b\alpha}(t'') = \int_0^{\hat{\omega}_1} d\omega\,\gamma_{\pi\pi\alpha}(t)g(t,t',t'')\omega^\beta\Theta(\omega) \quad (3.11)$$

and

$$\gamma_{\pi b(n)\alpha}(t,t')\gamma_{\pi b(n)\alpha}(t,t'') = \int_{\hat{\omega}_n}^{\hat{\omega}_{n+1}} d\omega\,\gamma_{\pi\pi\alpha}(t)g(t,t',t'')\omega^\beta\Theta(\hat{s}_0-s)\,, \quad (3.12)$$

where

$$\beta \equiv \alpha(t)-\alpha(t')-\alpha(t'')\,, \quad (3.13a)$$

$$\omega \equiv s + \tfrac{1}{2}(t-2m_\pi^2-t'-t'')\,, \quad (3.13b)$$

and $\hat{\omega}_n$ is the value of ω at $s=\hat{s}_n$, with $\hat{s}_n$ midway between $s_{b(n-1)}$ and $s_{b(n)}$ for $n\geq 1$.

The actual expressions for $\phi^2 a_2$ and its t derivative are, in general, rather complicated. They simplify considerably for $t=0$, however. In the above narrow-peak approximation, we then have

$$\phi^2 a_2(s,0) = \sum_{n,n'=0}^{\hat{N}} B_{nn'}(s,0)\Theta(s-s_0) \quad (3.14)$$

and

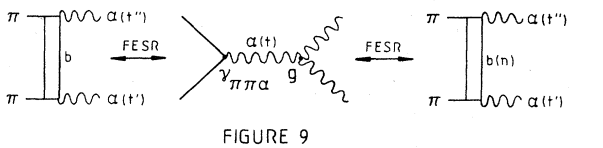

FIGURE 9

FIG. 9. Generalized finite-energy sum-rule duality of Eqs. (3.11) and (3.12).

$$\phi^2\left[\frac{\partial}{\partial t}a_2(s,t)\right]_{t=0}=\sum_{n,n'=0}^{\hat{N}}\left[\frac{\partial}{\partial t}B_{nn'}(s,t)\right]_{t=0}\Theta(s-s_0)\,, \tag{3.15}$$

where we have added a step function to prevent the double-counting of contributions which are already included in ϕa_1 and where

$$B_{nn'}(s,0)=\frac{K_{nn'}(0)}{16\pi s}\int_{t_-}^{t_+}dt'\,|\,T_{nn'}(t',0)\,|^2\Theta(s-(m_{b(n)}+m_{b(n')})^2)\,, \tag{3.16}$$

$$\left[\frac{\partial}{\partial t}B_{nn'}(s,t)\right]_{t=0}=\frac{K_{nn'}(0)}{16\pi s}\int_{t_-}^{t_+}dt'\left[\left[\frac{\partial}{\partial t}\,|\,T_{nn'}(t',t)\,|^2\right]_{t=0}-\frac{(t_+-t')(t_--t')}{s}\left|\frac{\partial}{\partial t'}T_{nn'}(t',0)\right|^2\right]$$
$$+\frac{1}{16\pi s}\left[\frac{\partial}{\partial t}K_{nn'}(t)\right]_{t=0}\int_{t_-}^{t_+}dt'\,|\,T_{nn'}(t',0)\,|^2\,, \tag{3.17}$$

with

$$T_{nn'}(t',t)=-\gamma_{\pi b(n)\alpha}(t',t)\gamma_{\pi b(n')\alpha}(t',t)\frac{e^{-i\pi\alpha(t')}}{\sin\pi\alpha(t')}[s+\tfrac{1}{2}(t'-m_{b(n)}{}^2-m_{b(n')}{}^2)]^{\alpha(t')}\,, \tag{3.18}$$

$$t_\pm=-\tfrac{1}{2}(s-m_{b(n)}{}^2-m_{b(n')}{}^2)\pm\tfrac{1}{2}\{[s-(m_{b(n)}-m_{b(n')})^2][s-(m_{b(n)}+m_{b(n')})^2]\}^{1/2}\,, \tag{3.19}$$

and

$$K_{nn'}(t)=1 \quad \text{if } n,n'<\hat{N} \tag{3.20a}$$

$$=\frac{\hat{s}_0(t)-\hat{s}_{\hat{N}}}{\hat{s}_{\hat{N}+1}-\hat{s}_{\hat{N}}} \quad \text{if } n=\hat{N},\ n'<\hat{N} \text{ or } n<\hat{N},\ n'=\hat{N} \tag{3.20b}$$

$$=\left[\frac{\hat{s}_0(t)-\hat{s}_{\hat{N}}}{\hat{s}_{\hat{N}+1}-\hat{s}_{\hat{N}}}\right]^2 \quad \text{if } n=n'=\hat{N}\,. \tag{3.20c}$$

As in Eq. (3.9), we have added in (3.16) the factor $K_{nn'}$—defined by (3.20)—to take into account the contribution between $\hat{s}_{\hat{N}}$ and $\hat{s}_0$, where $\hat{N}$ is such that $\hat{s}_{\hat{N}}<\hat{s}_0<\hat{s}_{\hat{N}+1}$.

Equations (3.11), (3.12), (3.7), and (3.6) relate all the couplings to $\gamma_{\pi a\pi}{}^2(t)$. The simplest approximation for $\gamma_{\pi a\pi}{}^2(t)$ would be to assume that it is dominated by the $J^P=1^-$ ρ resonance. However, this would not give rise to a nonsense wrong-signature zero at $\alpha(t)=0$ for $\gamma_{\pi b\alpha}{}^2(t')$, which is needed to cancel the pole arising at that point from the $\sin\pi\alpha(t')$ denominator in Eq. (3.18). We must therefore add in just the right amount of a $J^P=0^+$ contribution of the same mass (ϵ meson) so that $\gamma_{\pi a\pi}{}^2(t)\propto\alpha(t)$. According to this we set[11]

$$T_a(s,t)=\frac{1}{\pi}\frac{g_0}{m_\rho{}^2-s-i\gamma_0/2}+\frac{1}{\pi}\frac{3g_1(s)}{m_\rho{}^2-s-i\gamma_1/2}P_1(1+2t/s) \tag{3.21}$$

which, when combined with the identity

$$\frac{1}{m^2-s-i\gamma}=\mathrm{P}\frac{1}{m^2-s}+i\pi\delta(s-m^2) \tag{3.22}$$

(where P denotes that a principal-value integral is to be taken), gives

$$\mathrm{Im}T_a(s,t)=\left[g_0+3g_1(m_\rho{}^2)P_1\left[1+\frac{2t}{m_\rho{}^2}\right]\right]\delta(s-m_\rho{}^2)$$
$$\equiv\gamma_{\pi a\pi}{}^2(t)\delta(s-m_\rho{}^2)\,. \tag{3.23}$$

Now if we choose

$$g_0=3g_1(m_\rho{}^2)\,, \tag{3.24}$$

we can make, using Eq. (2.23),

$$\gamma_{\pi a\pi}{}^2(t)=12g_1(m_\rho{}^2)\alpha(t)\equiv\Gamma_0\alpha(t)\,. \tag{3.25}$$

Finally, Eqs. (3.25), (2.10), and (2.4), with $b_1b_2=\gamma_{\pi\pi\alpha}{}^2$, give

$$\gamma_{\pi\pi\alpha}{}^2(t)=\Gamma_0\alpha(t)[1+\alpha(t)]\bar{\nu}^{-(1+\alpha(t))}\,. \tag{3.26}$$

The dimensionless constant Γ_0 is the overall normalization of our couplings for any given t. Equation (3.26),

however, does not cancel the $\alpha(t)=-2,-3,..$ poles arising from the $\sin\pi\alpha(t')$ denominator in Eq. (3.18); so we must insert a cutoff, say, at $\alpha(t')=-1.5$, to exclude them. The region $\alpha(t')<-1.5$, though, should give a negligible contribution to our integrals. By modifying the procedure somewhat, this cutoff can be pushed any amount beyond $\alpha(t')=-1.5$ (Ref. 8).

If we now combine Eqs. (3.18) and (3.12), we get

$$|T_{nn'}(t',t)|^2=\gamma_{\pi\pi\alpha}{}^2(t)[\,|\tau_{nn'}(t',t)|^2-|\tau_{n+1,n'}(t',t)|^2-|\tau_{n,n'+1}(t',t)|^2+|\tau_{n+1,n'+1}(t',t)|^2\,]\,, \tag{3.27}$$

where

$$|\tau_{ll'}(t',t)|^2\equiv\frac{g^2(t',t',t)}{\sin^2\pi\alpha(t')}\frac{[s+\frac{1}{2}(t'-m_{b(n)}{}^2-m_{b(n')}{}^2)]^{2\alpha(t')}}{[1+\alpha(t)-2\alpha(t')]^2}[\hat{\omega}_l\hat{\omega}_{l'}]^{1+\alpha(t)-2\alpha(t')}\,, \tag{3.28}$$

with $\hat{\omega}_l$ and $\hat{\omega}_{l'}$ given by (3.13) at $t'=t''$ and $s=\hat{s}_l$ and $\hat{s}_{l'}$, respectively.

Equations (3.16) and (3.17) involve nonelementary integrals. However, each term in (3.27) falls off rapidly with t' for fixed t, so that we will approximate it by an exponentially damped function of the form

$$|\tau_{ll'}|^2=\tau_{0,ll'}e^{a_{ll'}t}e^{2c_{ll'}t'}\,, \tag{3.29}$$

where the constant $\tau_{0,ll'}$ is determined by demanding that the approximation be exact at $t=t'=0$; the coefficients $a_{ll'}$ and $c_{ll'}$ are fixed by requiring that the partial derivatives with respect to t and t', respectively, be exact at $t=t'=0$. We find the values

$$\tau_{0,ll'}=0.94\Gamma_0(\hat{s}_l\hat{s}_{l'})^{1/2}[s-\tfrac{1}{2}(m_{b(n)}{}^2+m_{b(n')}{}^2)]\,, \tag{3.30}$$

$$a_{ll'}=-1.42+\frac{0.25}{\hat{s}_l}+\frac{0.25}{\hat{s}_{l'}}+0.83\ln(\hat{s}_l\hat{s}_{l'})\,, \tag{3.31}$$

$$c_{ll'}=-a_{ll'}+\frac{0.25}{s-\frac{1}{2}(m_{b(n)}{}^2+m_{b(n')}{}^2)}+0.83\ln[s-\tfrac{1}{2}(m_{b(n)}{}^2+m_{b(n')}{}^2)]\,. \tag{3.32}$$

If we take the Mellin transform (2.1) of $\phi a_1(s,t)$—given by (3.9)—and $\phi^2 a_2(s,t)$, and insert them into Eq. (3.1), we have

$$K(j,t)=\left[\sum_{n=0}^{N}K_n\gamma_{\pi a(n)\pi}{}^2(t)\nu_{a(n)}{}^{-j-1}\right]^{-1}\times\int_0^\infty ds\,\phi^2 a_2(s,t)\nu^{-j-1}\,. \tag{3.33}$$

Finally, if we impose the constraints (3.2)–(3.5) on (3.33)—using (3.14), (3.15), (3.16), (3.17), (3.27), (3.29), (3.7), (3.6), and (3.25)—we obtain the following values for our unknowns,

$$s_0=3.27\ \text{GeV}^2,\quad \hat{s}_0=4.0\ \text{GeV}^2,\quad \hat{s}_0'(0)=-1.1\,, \tag{3.34}$$

and

$$\Gamma_0=206.65\,. \tag{3.35}$$

There is no direct unambiguous way of comparing these values with experiment. In the next two sections, however, we will consider a confrontation with experiment through the calculations of the triple-Regge coupling constant and partial widths.

C. An alternative calculation assuming a dual-tree-model form for the triple-Regge coupling

One way of avoiding altogether the $\alpha(t')=-1.5$ cutoff discussed in the last section is to assume that the triple-Regge coupling g is determined by a dual-tree model of the Neveu-Schwartz type, which gives

$$g^2(t,t',t')=N\bar{g}^2\frac{\Gamma(\alpha(t))\Gamma^2(1-\alpha(t'))}{\Gamma^2(1+\alpha(t)-2\alpha(t'))}\sin^2\pi\alpha(t')\,, \tag{3.36}$$

where $\bar{g}$ is a dimensionless coupling constant and N is the number of quarks. If we assume that SU(3) is the underlying group, $N=3$. The use of Eq. (3.36) for g is an alternative to the expressions (3.11) and (3.26), obtained by imposing semilocal duality and assuming (3.25).

Now $|\tau_{ll'}(t',t)|^2$ is determined by the Eqs. (3.28) and (3.36). It again falls off rapidly with t' for fixed t and so we will use the exponential approximation (3.29), where, in the present case, we have

$$\tau_{0,ll'}=4\pi^{1/2}N\bar{g}^2(\hat{s}_l\hat{s}_{l'})^{1/2}[s-\tfrac{1}{2}(m_{b(n)}{}^2+m_{b(n')}{}^2)]\,, \tag{3.37}$$

$$a_{ll'}=-1.69+\frac{0.25}{\hat{s}_l}+\frac{0.25}{\hat{s}_{l'}}+0.83\ln(\hat{s}_l\hat{s}_{l'})\,, \tag{3.38}$$

$$c_{ll'}=-a_{ll'}+\frac{0.25}{s-\frac{1}{2}(m_{b(n)}{}^2+m_{b(n')}{}^2)}+0.83\ln[s-\tfrac{1}{2}(m_{b(n)}{}^2+m_{b(n')}{}^2)]\,, \tag{3.39}$$

and the numerical outcomes are

$$s_0=4.7\ \text{GeV}^2,\quad \hat{s}_0(0)=5.5\ \text{GeV}^2,\quad \hat{s}_0'(0)=-0.7\,, \tag{3.40}$$

and

$$N\bar{g}^2/16\pi=0.58\ . \tag{3.41}$$

The couplings Γ_0 and $N\bar{g}^2/16\pi$ can be related to each other through the corresponding expressions for $g^2(0,0,0)$. So at $t=t'=t''=0$, Eqs. (3.11) with $b=\pi$ and (3.26) reduce to

$$g^2(0,0,0)=\frac{\Gamma_0\alpha(0)[1+\alpha(0)][1-\alpha(0)]^2}{(\hat{s}_1)^{2-2\alpha(0)}(\bar{s}_1)^{1+\alpha(0)}}\ , \tag{3.42}$$

which, when compared with (3.35), gives

$$N\bar{g}^2/16\pi=\Gamma_0/377.90\ , \tag{3.43}$$

where we used the values $\alpha(0)=0.5$, $\bar{s}_1=m_\rho^2+(2\alpha')^{-1}=1.204$ GeV^2, and $\hat{s}_1=m_\pi^2+(2\alpha')^{-1}=0.602$ GeV^2. If we now insert the result (3.41) into (3.43), we get

$$\Gamma_0=219.18\ . \tag{3.44}$$

On the other hand, the triple-Regge coupling constant, obtained with the semilocal-duality model (3.35), is

$$N\bar{g}^2/16\pi=0.55\ , \tag{3.45}$$

which is in turn rather close to the dual-tree value (3.41). Both values should be compared with the "experimental" estimate $N\bar{g}^2/16\pi\sim 1$ obtained in Refs. 16 and 17. However, this experimental estimate relies heavily on a version of the two-component duality hypothesis of Freund and Harari[18] which may not be very good. In the next section we will make a less ambiguous comparison with experiment.

D. Calculation of meson resonance widths

Partial widths are another kind of coupling which can be calculated within our approach. For simplicity, we shall continue considering only $\pi\pi$ scattering.

If we make the t-channel partial-wave projection (2.1) of $\gamma_{\pi\pi\alpha}{}^2\nu^\alpha$, we obtain a resonance of spin j at $t=t_j$ if $\alpha(t_j)=j$. With $m_\pi{}^2\simeq 0$, the corresponding partial width in the energy ($\sqrt{t}$) variable is then given by

$$\gamma_j=\frac{2^j(j+1)(j!)^2}{(2j+1)(2j)!}\left[\frac{t_j}{2\bar{s}+t_j}\right]^{j+1}\frac{1}{8\pi^2\alpha'}\frac{\Gamma(t_j)}{t_j{}^{3/2}}\ , \tag{3.46}$$

where we shall assume

$$\Gamma(t)=\Gamma_0\alpha(t)\ . \tag{3.25'}$$

Equation (3.46) applies to the ordered planar amplitude $T(s,t)$ which only has s-t crossing. For $\pi\pi$ scattering, the full planar amplitude for the t-channel isospin $I_t=0,1$ states is[11]

$$T^0=\tfrac{3}{4}[T(t,s)+T(t,u)]-\tfrac{1}{4}T(s,u)\ , \tag{3.47a}$$

$$T^1=\tfrac{1}{2}[T(t,s)-T(t,u)]\ . \tag{3.47b}$$

Thus

$$\text{total partial width}=\begin{cases}\tfrac{3}{2}\gamma_j, & I_t=0\ , \quad (3.48a)\\ \gamma_j, & I_t=1\ . \quad (3.48b)\end{cases}$$

If we combine Eqs. (3.46), (3.25'), and (3.48), with Γ_0 given by Eq. (3.35), and if we use semilocal duality for g, we get

$$\begin{aligned}&\gamma_\rho=\gamma_1=0.18\text{ GeV},\quad \gamma_f=\tfrac{3}{2}\gamma_2=0.12\text{ GeV}\ ,\\ &\gamma_g=\gamma_3=0.04\text{ GeV},\quad \gamma_h=\tfrac{3}{2}\gamma_4=0.03\text{ GeV}\ ,\end{aligned} \tag{3.49}$$

while, with the dual-tree result (3.44), we end up with

$$\begin{aligned}&\gamma_\rho=\gamma_1=0.19\text{ GeV},\quad \gamma_f=\tfrac{3}{2}\gamma_2=0.13\text{ GeV}\ ,\\ &\gamma_g=\gamma_3=0.04\text{ GeV},\quad \gamma_h=\tfrac{3}{2}\gamma_4=0.03\text{ GeV}\ .\end{aligned} \tag{3.50}$$

Equations (3.49) and (3.50) should be compared with the experimental ρ-, f-, and g-meson $\pi\pi$ partial decay widths

$$\begin{aligned}&\gamma_\rho=0.154\pm 0.005\text{ GeV}\ ,\\ &\gamma_f=0.149\pm 0.017\text{ GeV}\ ,\\ &\gamma_g=0.048\pm 0.005\text{ GeV}\ .\end{aligned} \tag{3.51}$$

We see that the values we obtain are in good agreement with experiment. In the case of f and h, we should keep in mind that the widths are modified by nonplanar cylinder corrections.[3] We can also calculate the $\pi\pi$ partial decay widths of resonances beyond g and h. We get, for instance, the values $\gamma_5=0.01$ GeV and $\frac{3}{2}\gamma_6=0.01$ GeV with both models.

IV. SUMMARY

We have considered the dual topological unitarization (DTU) approach to the study of strong interactions. DTU provides us with a quasiperturbative expansion based on the topology of quark-duality diagrams generated by unitarity. Unlike many other approaches, DTU takes sea-quark loops into account from the beginning. This strong-coupling method is particularly suitable for the description of low-momentum-transfer interactions.

The leading term consists of all planar diagrams, which have the simplest topologies and give a good first approximation to the soft-hadron physics. They satisfy a nonlinear consistency equation, known as planar unitarity. The solution of this planar bootstrap problem is the first step in the DTU program. Once we have its solution, nonplanar effects can be systematically brought in through the topological expansion.

In Sec. II we reviewed the planar bootstrap technique developed by Balázs, in which finite-energy sum rules are combined with an infinite sum of ladder graphs generated by unitarity. By making a certain simple dynamical approximation, the bootstrap problem is solved and a simple linear form for the leading Regge trajectory $\alpha(t)$ is obtained.

In Sec. III we considered, within the same approach as in Sec. II, a model for making coupling calculations at and near $t=0$, where the scattering amplitude takes on a particularly simple form. We approximated the ladder exchanges by Regge exchanges and assumed that the [1,1] Padé approximant was a good representation of the absorptive part of the amplitude. The practical advantage of using this approximant was that we only had to evalu-

ate the first two diagrams of the infinite sum of ladder graphs, namely, the resonance and the box graphs. In the case of factorizable models, the [1,1] Padé approximant is exact. Our computations were restricted to $\pi\pi$ scattering, although our methods are applicable to any multiquark system. By making narrow-peak approximations to the resonance clusters that appear in both graphs and using semilocal duality, we were able to solve our dynamical equations and obtain the cutoffs of the clusters and the overall normalization constant of our couplings. We compared the results with similar calculations based on a dual-tree model of the Neveu-Schwartz type. We calculated the triple-Regge coupling constant and the widths of the meson resonances, which are close to the experimental values.

ACKNOWLEDGMENTS

This work was done while the author was at Purdue University, West Lafayette. He is very grateful to Professor L. A. P. Balázs for proposing these calculations and for many valuable suggestions and comments. The partial financial assistance provided by Departamento de Investigaciones Científicas y Tecnológicas, Universidad de Santiago de Chile, is gratefully acknowledged.

[1]K. G. Wilson, Phys. Rev. D **10**, 2445 (1974); G. 't Hooft, Nucl. Phys. **B72**, 461 (1974); R. Brower, R. Giles, and C. Thorn, Phys. Rev. D **18**, 484 (1978).

[2]A. Chodos and C. B. Thorn, Phys. Rev. D **12**, 2733 (1975); T. Inoue and T. Maskawa, Prog. Theor. Phys. **54**, 1833 (1975); G. E. Brown and M. Rho, Phys. Lett. **82B**, 177 (1979); S. Théberge, A. W. Thomas, and G. A. Miller, Phys. Rev. D **22**, 2838 (1981); **24**, 216 (1981).

[3]G. F. Chew and C. Rosenzweig, Phys. Rep. **41**, 263 (1978); L. Montanet, G. C. Rossi, and G. Veneziano, *ibid.* **63**, 149 (1980).

[4]G. F. Chew and V. Poénaru, Z. Phys. C **11**, 59 (1981).

[5]H. P. Stapp, Phys. Rev. D **27**, 2445 (1983); **27**, 2478 (1983).

[6]C. Rosenzweig and G. Veneziano, Phys. Lett. **52B**, 335 (1974).

[7]L. A. P. Balázs, Phys. Lett. **120B**, 426 (1983).

[8]L. A. P. Balázs, Phys. Rev. D **26**, 1671 (1982).

[9]L. A. P. Balázs, Phys. Lett. **71B**, 216 (1977).

[10]L. A. P. Balázs, Phys. Rev. D **20**, 2331 (1979).

[11]P. D. B. Collins, *An Introduction to Regge Theory and High Energy Physics* (Cambridge University Press, Cambridge, England, 1977).

[12]G. A. Baker, Jr., *Essentials of Padé Approximants* (Academic, New York, 1975).

[13]L. A. P. Balázs and B. Nicolescu, Phys. Lett. **72B**, 240 (1977).

[14]L. A. P. Balázs and B. Nicolescu, Z. Phys. C **6**, 269 (1980).

[15]L. A. P. Balázs, Phys. Lett. **99B**, 481 (1981).

[16]Chang Hong-Mo, J. E. Paton, and Tsou Sheung Tsun, Nucl. Phys. **B86**, 479 (1975).

[17]L. A. P. Balázs, Phys. Rev. D **15**, 319 (1977).

[18]H. Harari, Phys. Rev. Lett. **20**, 1395 (1968); P. G. O. Freund, *ibid.* **20**, 235 (1968).